

# DESIGN, PRODUCTION AND BIOCOMPATIBILITY OF NANOSTRUCTURED POROUS HAp AND Si-HAp CERAMICS AS THREE-DIMENSIONAL SCAFFOLDS FOR STEM CELL CULTURE AND DIFFERENTIATION

GIORGIA LEHMANN, PAOLA PALMERO\*, ILARIA CACCIOTTI\*\*, RAFFAELLA PECCI\*\*\*, LUISA CAMPAGNOLO, ROSSELLA BEDINI\*\*\*, GREGORIO SIRACUSA, ALESSANDRA BIANCO\*\*, ANTONELLA CAMAIONI, LAURA MONTANARO\*

*Department of Public Health and Cell Biology, University of Rome Tor Vergata, Rome, Italy*

*\*Department of Materials Science and Chemical Engineering, Politecnico di Torino, Turin, Italy*

*\*\* Department of Chemical Science and Technology, University of Rome Tor Vergata, Rome, Italy*

*\*\*\* Department of Technology and Health, Istituto Superiore di Sanità, Rome, Italy*

E-mail: camaioni@uniroma2.it

Submitted December 8, 2009; accepted March 12, 2010

**Keywords:** Silicon-substituted hydroxyapatite, Embryonic stem cell, Osteoclast, Nano-structured porous scaffold

*Biocompatible and biodegradable scaffolds can provide a convenient support for stem cell differentiation leading to tissue formation. Porous hydroxyapatite (HAp) scaffolds are clinically used for applications such as spinal fusions, bone tumors, fractures, and in the replacement of failed or loose joint prostheses. The incorporation of small amounts of silicon within hydroxyapatite lattice significantly improves HAp solubility and rate of bone apposition, as well as the proliferation of human osteoblasts in vitro. In the present paper we report biocompatibility data obtained on a newly designed three-dimensional nano-structured porous scaffold made of pure and silicon-substituted hydroxyapatite. A suitable amount of porosity (60 vol%) was obtained within a well densified ceramic skeleton by using polyethylene spheres. Biocompatibility was tested by using murine embryonic stem cells (ES). Cell culture analysis indicated that ES cells adhere well on both hydroxyapatite and silicon-substituted hydroxyapatite scaffolds. Si-substitution, however, improved subsequent ES cell proliferation rate. Bioresorption of hydroxyapatite scaffolds was tested by using human osteoclasts obtained from peripheral blood monocytes, made to differentiate on disks and evaluated by SEM analysis.*

## INTRODUCTION

Biomimetic material supports may be used to provide stem cells with appropriate environmental cues influencing gene expression and differentiation, with the aim to *in vitro* mimic tissue growth. Various approaches have been reported in the literature to show that many tissues may be regenerated by stem cells growing on biomaterials [1].

Scaffolds used for tissue engineering should have the following characteristics: biocompatibility, biodegradability, reproducibility, high porosity with interconnection pores, and no potential of serious immunological or foreign body reaction. Moreover, depending on the tissue type, they should promote secretion of extracellular matrix molecules and carry biomolecular signals [1]. In particular, for bioceramic implants, the incorporation of silicon (Si) within the hydroxyapatite (HAp) lattice has been shown to significantly improve HAp solubility and rate of bone apposition, as well as to enhance the proliferation of

human osteoblasts *in vitro* [2]. Furthermore, biological studies and clinical practice have highlighted that, in addition to compositional requirements, a three-dimensional interconnected porous structure improves tissue development and provides temporary mechanical support [3, 4].

The aim of the present study was to design biocompatible porous ceramic scaffolds that might facilitate stem cell differentiation and tissue formation. We first tested the biocompatibility of the scaffolds by an adaptation of the EST test [5], *i.e.* by evaluating scaffolds ability to support the growth of murine embryonic stem cells (ES cells), cell lines that are very sensitive to suboptimal environmental changes [6]. Bone is a dynamic tissue that constantly undergoes turnover (bone remodelling) in order to maintain stability and integrity, and two effector cell types are involved in this process: osteoblasts, responsible for bone formation and osteoclasts, specialized for bone resorption [7]. Measuring bioresorption of ceramic scaffolds by osteoclasts should provide information in the perspective

of implanting these scaffolds into patients. Human osteoclasts, derived from the differentiation of peripheral blood monocytes, were seeded on not porous scaffolds in order to analyse their resorption activity.

## MATERIALS AND METHODS

### Pure and Si-substituted hydroxyapatite three-dimensional porous scaffold production

Three-dimensional nanostructured porous scaffolds made of pure and silicon-substituted hydroxyapatite (11 mm diameter, 3 mm height disks) have been produced as follows. Pure (HAp) and Si-substituted (Si-HAp) hydroxyapatite powders were synthesized in a double-walled jacket reactor at 40°C under magnetic stirring by titration of 10 g/l aqueous suspension of calcium hydroxide (Ca(OH)<sub>2</sub>, Aldrich 99.5 %, MW 74.10) with phosphoric acid solution (H<sub>3</sub>PO<sub>4</sub>, Aldrich 86.3 %, MW 98.00). In order to obtain 1.4 wt. % Si-HAp, tetraethyl orthosilicate (TEOS, Si(OC<sub>2</sub>H<sub>5</sub>)<sub>4</sub>, Aldrich 99.99 %, MW 208.33) was added to the phosphoric acid solution, prior to the titration with the calcium hydroxide suspension. For both samples, the pH was finally adjusted to 9.4.

Precipitates were aged in mother liquor at room temperature for 24 hours, washed with NH<sub>4</sub>OH aqueous solution, vacuum filtered and finally dried in oven at 60°C (*as-dried* samples) [8].

Freshly synthesized nanopowders were planetary milled for 1 hour. After drying, milled powders were calcined at 600°C for 1 hour, to prevent relevant weight losses during the densification process and then mixed with commercially available polyethylene spheres (PE, Clariant Italia SpA) used as porogen. PE, sieved in the range 355-420 µm, was added in amount to obtain a porosity of 60 vol.% in the fired materials. Green pellets were obtained by cold uniaxial pressing at 25 MPa and then submitted to controlled thermal cycles to firstly decompose the organic matter and then sinter (up to 1150°C for 3 hours) the ceramic skeleton.

### Characterisation

Microstructural features of *as-dried* powders were studied by Transmission Electron Microscopy (TEM) (Philips CM120) in bright field mode, the accelerating voltage being 100 kV. Samples for TEM investigation were prepared as follows. Both HAp and Si-HAp *as-dried* powders were dispersed in distilled water by ultrasonication for about 30 minutes and a drop of the suspensions was then picked up with copper meshes having carbon film coating.

X-ray diffraction (XRD) (Philips X'Pert 1710) (Cu K<sub>α</sub> radiation λ=1.5405600 Å, 20-55° 2θ, step size 0.010°, time per step 2 s, scan speed 0.005°/s) analyses were performed on both *as-dried* and calcined powders at different temperatures up to 1400°C.

On the grounds of TG-DTA and XRD analyses, powders were pre-treated at 600°C for 1 hour (heating and cooling rate of 10°C/min) to prevent relevant weight losses during the densification process. Bars were cold uniaxially pressed at 400 MPa and dilatometric analyses (Netzsch 402E) were performed in the following conditions: peak temperature 1250°C, soaking time 1 hour, heating and cooling rate 10°C/min [8].

Micro-computerized tomographic analysis (Skyscan 1072, SKYSCAN, Kontich, Belgium) of the obtained reconstruction three-dimensional porous scaffold images was performed in order to evaluate pore size distribution and open porosity percentage by means of *Cone\_rec*, *3D\_creator* and *CT\_An* processing softwares [9]. Total porosity is the volume of all open plus closed pores as a percentage of the total volume of interest (VOI). In the 3D calculation, volumes are calculated on the basis of the *Marching Cubes* algorithm that has a repertoire of surface voxel architectures each with a calculated percent object volume [10].

### Murine ES cell culture

Mouse ES cells (line D3) were cultured following standard procedures [11] on a feeder layer of mitotically-inactivated primary murine embryonic fibroblasts (MEFs) obtained from CD-1 mouse embryos, on gelatin coated tissue culture plates (CPs). The same procedure was used when testing experimental scaffolds. ES cells were expanded and maintained undifferentiated by culture in Dulbecco's Modified Eagle's Medium (DMEM with 4.5 g/L D-glucose) supplemented with 15 % heat-inactivated fetal calf serum (ES cell tested), 20 mM HEPES, 2 mM L-glutamine, 100 µM β-mercaptoethanol, 100 µM non-essential amino acids, 50 U/ml penicillin and 50 µg/ml streptomycin (all from Lonza, Switzerland), and 10<sup>3</sup> U/ml Leukemia Inhibitory Factor (LIFES, Immunological Sciences, Italy). The cells were cultured at 37°C in a humidified atmosphere of 5 % CO<sub>2</sub> in air. To obtain highly enriched ES cell populations, cultures reaching 80 % confluency were trypsinized and gently disaggregated by pipetting. After centrifugation, cells were suspended in culture medium and plated onto CPs for 20–40 minutes in the incubator. During this time, MEFs attach to the plate while ES cells remain suspended in the supernatant and could be harvested for subsequent use. Before each experiment, scaffolds were washed in 18 MΩ water, air-dried and heat sterilized. MEFs were then seeded on the scaffolds and on standard CPs and incubated overnight. The next day, ES cells were seeded in each well in 600 µl of medium, at the concentration of 13000 cells/cm<sup>2</sup>. For cell viability experiments, 100000 ES cells were seeded on the scaffolds and on standard CPs and 6 hours later the medium with non-adhering cells was removed. The viability of non-adhering ES cells was evaluated through trypan blue (Sigma, MO, USA) dye exclusion test.

### Human osteoclast cell culture

Buffy coat cells, obtained from the blood of healthy donors were diluted 1:1 with  $\alpha$ -MEM, (Lonza, Switzerland), transferred to tubes containing Ficoll-Paque Plus (GE Healthcare, Sweden) and centrifuged (400 g, 40 min) to obtain peripheral blood mononuclear cells (PBMCs) [12] enriched in monocytes, platelets, and lymphocytes. The cells were washed and suspended in  $\alpha$ -MEM with 10 % (v/v) fetal calf serum, and finally cultured at a concentration of  $2.5 \times 10^6$  cells/cm<sup>2</sup> on tissue culture plates. After overnight culture, non-adherent cells were removed and 600  $\mu$ l of medium containing 50 ng/ml of monocyte colony stimulating factor (M-CSF, Immunological Sciences, Italy) was added. After reaching confluency (6-8 days in most cases), the cells were cultured in the presence of 50 ng/ml Receptor Activator for Nuclear Factor  $\kappa$  B Ligand (RANK-L, Immunological Sciences, Italy) and 20 ng/ml M-CSF. Medium was replaced every 3 days. After three weeks of culture the samples were washed with PBS, and the cells were fixed and stained for tartrate resistant alkaline phosphatase (TRAP) (Sigma-Aldrich, Poole, UK). For Scanning Electron Microscope (SEM) analysis of HAp bioresorption, scaffolds cultured with or without cells and scaffolds cleared of the cells by trypsinization, were fixed in 2.5 % glutaraldehyde, dehydrated through a graded series of ethanol up to absolute and analyzed by SEM (Hitachi H-7100FA), after gold sputter-coating, to detect the presence of resorption pits.

### MTT assay

ES cell adhesion was evaluated 16 hours after seeding 25000 ES cells on scaffolds and on CPs, by a modification of the methylthiazolyldiphenyl-tetrazolium bromide (MTT; Sigma, MO, USA) assay [13]. Parallel cultures without ES cells (MEFs only) were also analyzed, in order to subtract the background due to the feeder layer. Briefly, each sample was incubated at 37°C for 1 hour with 0.5 mg/ml MTT solution (600  $\mu$ l/well). The MTT solution was then removed and dimethylsulfoxide (Sigma, MO, USA) (450  $\mu$ l/well) and glycine buffer (pH = 10.5, 62.5  $\mu$ l/well) were added to each well. After 10 min of agitation, the absorbance at 540 nm was measured with a SmartSpec 3000 spectrophotometer (Bio-Rad, CA, USA).

## RESULTS AND DISCUSSION

### Scaffold structure

Semicrystalline, nano-sized (10-20 nm width and 50-200 nm length), needle-like particles were obtained (Figure 1a). Samples consisted of single phase HAp up

to 1300°C (HAp) and 1200°C (Si-HAp), respectively (Figure 1b). Pure HAp showed shrinkage onset temperature at 800°C and maximum sintering rate temperature at about 1050°C. A linear shrinkage of about 18 % was almost completely recovered during heating. Si-HAp was characterized by a displacement of sintering temperatures to higher values (Figure 1c).

HAp and Si-HAp porous scaffolds showed an actual porosity of about 58 % and 49 %, respectively. Pore average diameter (Figure 1d) was larger in the Si-HAp scaffold (600  $\mu$ m) than in the HAp one (320  $\mu$ m). The average diameter of pores was obtained by the value of the structure separation (St.Sp) in 3D morphometric analysis calculated by the *Skyscan CT-analyser* software. Structure separation is essentially the thickness of the spaces as defined by binarisation within the VOI; it is possible to measure St.Sp directly and model-independently in 3D by the same method used to measure structure thickness [14], just applied to the space rather than the solid voxels.

### Scaffold biocompatibility

We evaluated the HAp and Si-HAp scaffolds biocompatibility by monitoring embryonic stem cells culture behaviour. We analyzed murine embryonic stem cell adhesion, viability of non-adhering cells and proliferation (Figure 2), using standard culture plates (CP) as control.

ES cell adhesion rate, measured by MTT assay 16 hours after seeding the cells, was  $40.5 \pm 4.4$  % on HAp and  $29.8 \pm 4.2$  % on Si-HAp, as compared to control cultures (Figure 2a). Non-adhering ES cell viability was analyzed by Trypan blue dye exclusion test at 6 hours after seeding (Figure 2a, inset) and the result showed that neither scaffold interfered with cell viability. Finally, the proliferation rate of the ES cells cultured for additional 24 hours, that is a total of 40 hours of culture, was not different from that seen in control cultures in the case of Si-HAp, while it was slower on HAp (Figure 2b).

Therefore murine embryonic stem cells show similar adhesion properties but different proliferation rates on HAp and Si-HAp scaffolds. In fact, the silicon substitution within hydroxyapatite seems to improve ES cells proliferation. These results should be confirmed by further experiments on osteoblast-like cells in order to verify whether the Si-HAp increases osteoblast proliferation and bone matrix apposition as already reported in the literature [2].

### Scaffold bioresorption

To test the ability of HAp and Si-HAp scaffolds to undergo bioresorption we cultured human osteoclasts, obtained through the differentiation of monocyte precursors isolated from human peripheral blood. The cells were seeded on non-porous HAp scaffolds. When



confluence was reached, the cells were treated with 50 ng/ml RANK-L and 20 ng/ml M-CSF for about 21 days, until mature osteoclasts formed. The presence of mature osteoclasts was confirmed by both morphological analysis (presence of multinucleated cells) (Figure 3a) and TRAP staining (Figure 3b) on parallel cultures on tissue culture plates.

Bioresorption was evaluated by osteoclasts capability to form resorption pits (Howship lacunae) on the surface of non-porous HAp disks, as shown by SEM analysis after removing the cells by trypsinization (Figure 4). HAp scaffolds have good bioresorption properties as shown by osteoclasts activity (formation of resorption pits) on the disks. This suggests that these materials

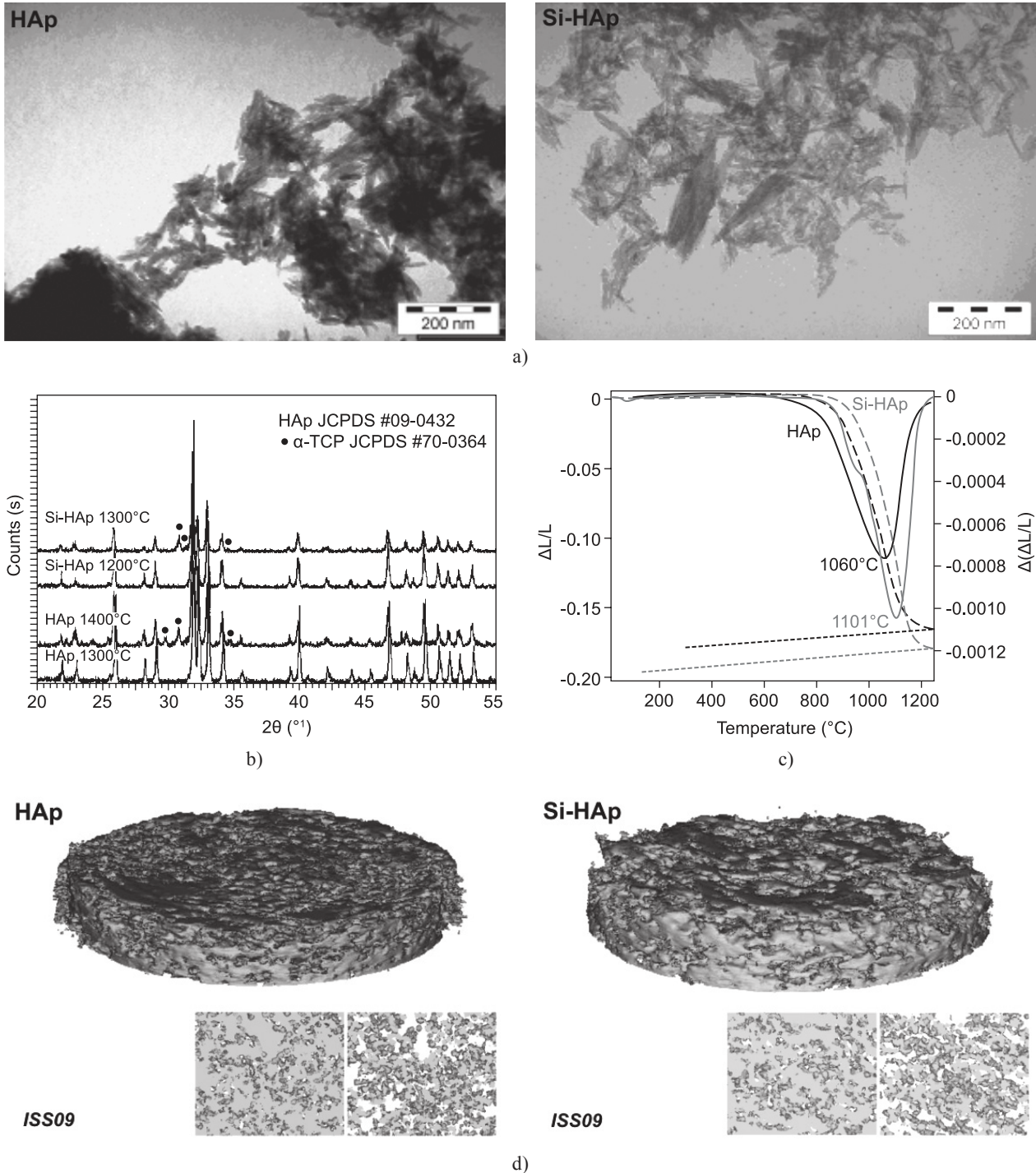


Figure 1. a) TEM images of as dried HAp and Si-HAp nanopowders. b) XRD spectra of HAp and Si-HAp powders calcined at different temperatures. c) Dilatometric (dotted line) and derivative (solid line) curves of HAp and Si-HAp powders. d) 3D X-ray micro-computed tomography images of HAp and Si-HAp porous scaffolds and longitudinal slices (left) with interconnectivity image (right) for each sample.

could be suitable for long-term implants as they promote bone turnover, not only by stimulating cell proliferation, but also by promoting bone resorption by osteoclasts.

### CONCLUSIONS AND FUTURE PERSPECTIVES

In this study, nano-structured porous ceramic scaffolds were successfully produced by pressing a mixture of HAp powders (pure or Si-substituted) with commercially available PE spheres. After a controlled thermal treatment, a suitable amount of porosity (60 vol.%) was obtained into a well densified ceramic skeleton.

Cell culture analysis indicated that ES cells adhere well on both HAp and Si-HAp scaffolds. Si-substitution, however, improved ES cell proliferation rate. Finally, bioresorption of HAp scaffolds was tested

by using human osteoclasts differentiated on disks from peripheral blood monocytes and evaluated by SEM analysis. Simulating bone turnover *in vitro* on a scaffold is an important step to evaluate its possible use in a clinical context to regenerate a complex and dynamic tissue such as bone. Further studies are ongoing to test adhesion and proliferation on both scaffolds of pre-osteoblasts from murine neonatal cranial bones. This cell type has been chosen in the prospect to differentiate it into mature osteoblasts that are responsible for bone formation. Furthermore, gene expression studies will be necessary to verify the effect of scaffolds on osteoblast differentiation and their possible use in bone tissue engineering. Likewise, *in vivo* implants of seeded scaffolds in mice might provide relevant information on their potential use in the field of regenerative medicine.

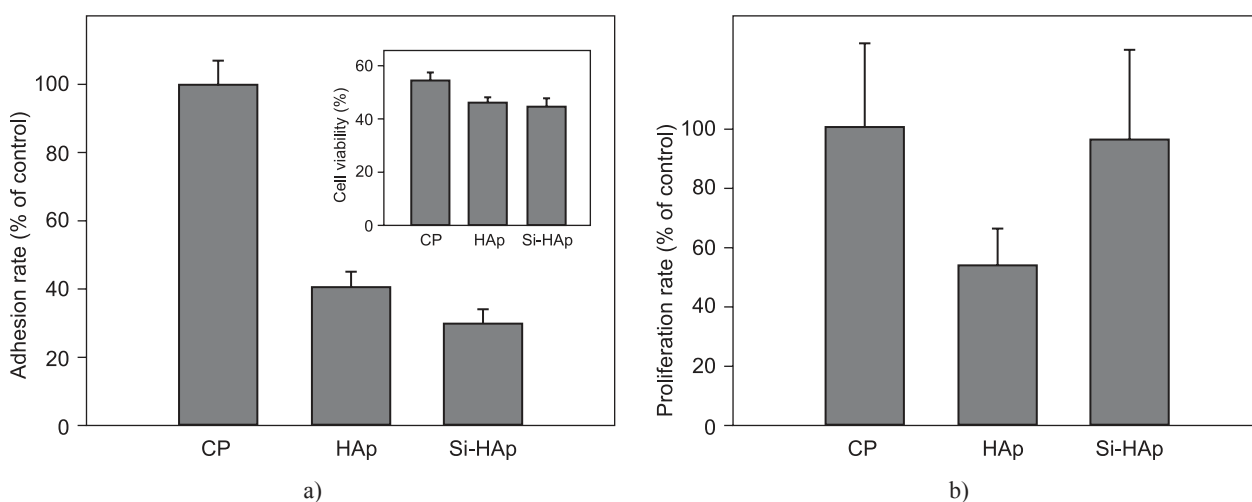


Figure 2. Murine embryonic stem cell adhesion and proliferation. a) Adhesion, measured by MTT assay 16 hours after seeding the cells in standard conditions on tissue culture plates (CP) and on HAp and Si-HAp scaffolds. Results are expressed as percentage of the standard culture (CP = 100%). Inset: Scaffold effects on the viability of non-adhering cells, evaluated by Trypan blue dye exclusion test at 6 hours after seeding. b) Proliferation, measured by MTT assay 40 hours after seeding the cells in standard conditions on tissue culture plates (CP) and on HAp and Si-HAp. Results are expressed as percentage of the standard culture (CP = 100%). Values represent mean  $\pm$  standard error from three independent experiments performed in triplicate.

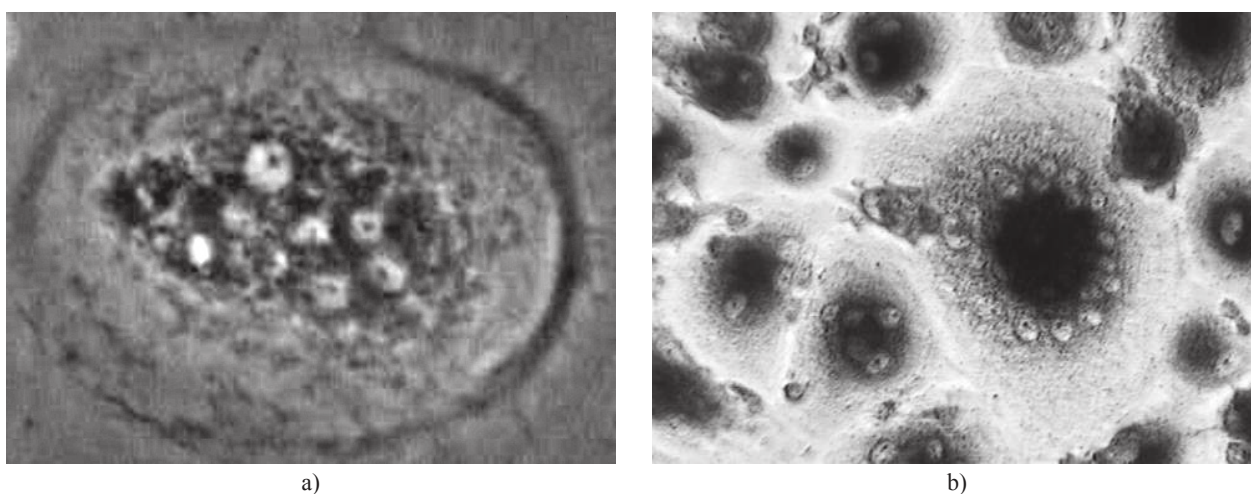


Figure 3. a) Phase contrast micrograph of a mature osteoclast on CP. b) Mature osteoclasts and osteoclast precursors cultured on CP, stained by TRAP.



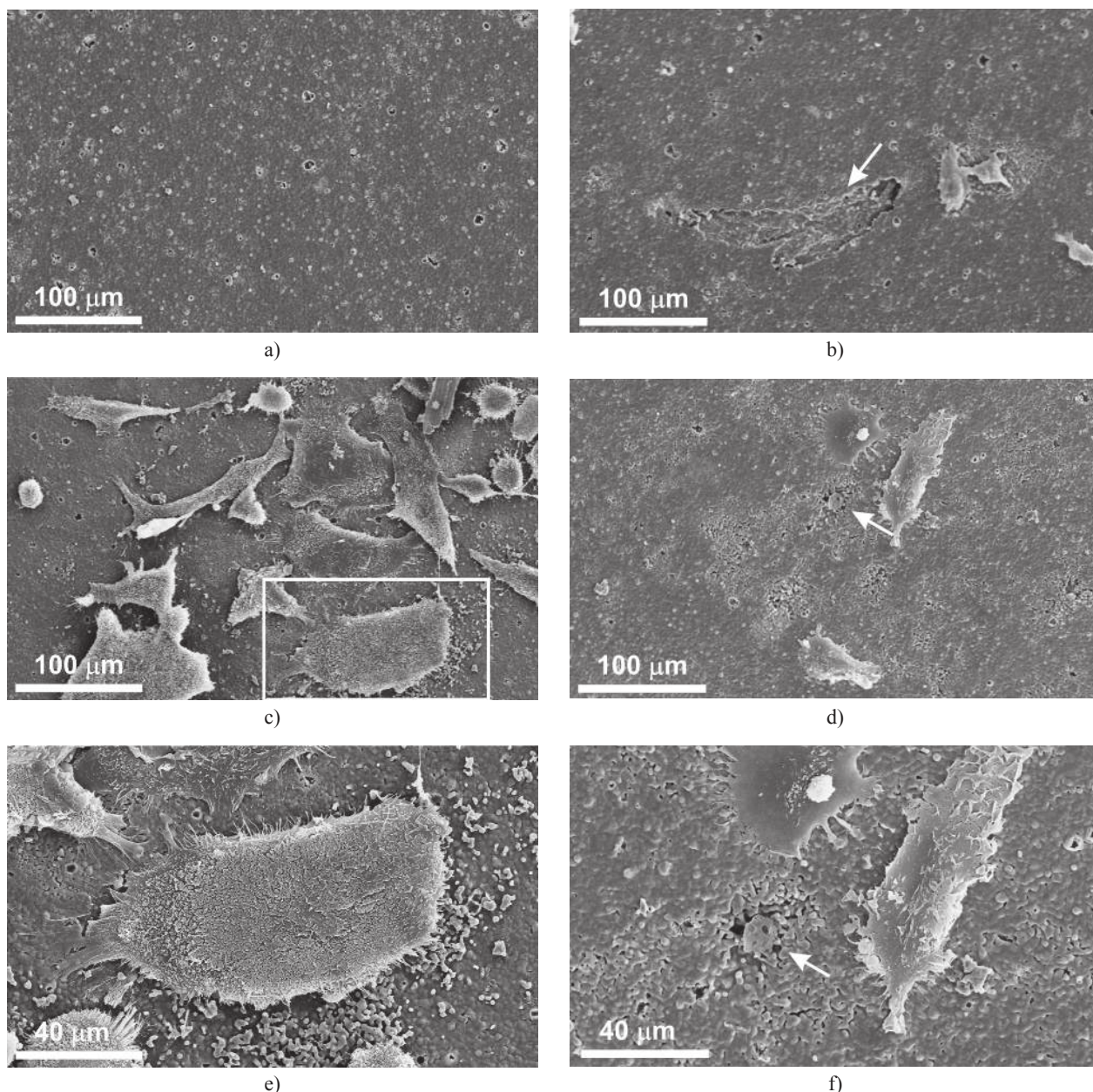


Figure 4. SEM of non-porous HAp scaffolds not seeded (a) or seeded (b-f) with human monocytes differentiated into osteoclasts. c) Cells cultured on a HAp scaffold (red square shows a putative osteoclast, seen at higher magnification in e). Following removal of most cells by trypsinization (b, d, f), resorption lacunae (red arrows) can be observed (f) is a higher magnification of (d).

#### Acknowledgements

The Authors would like to acknowledge Prof. E. Bemporad and Mr. D. De Felicis, University of Rome Roma Tre, Rome, Italy for TEM analysis and Dr. A. Volpe, University of Rome Tor Vergata, Rome, Italy for SEM analysis. A special thank to Mr G. Bonelli for expert graphic assistance.

This work has been supported by PRIN2006 Project titled "Design and realization of organic, inorganic and hybrid nanostructured scaffolds as substrates for the differentiation of stem cells in regenerative medicine".

#### References

1. Liao S., Chan C. K., Ramakrishna S.: *Mater.Sci.Eng. C* 28, 1189 (2008).
2. Pietak M. A., Reid J. W., Scott M. J., Sayer M.: *Bio-materials* 28, 4023 (2007).
3. Cancedda R., Giannoni P., Mastrogiacomo M.: *Bio-materials* 28, 4240 (2007).
4. Yoshikawa H., Tamai N., Murase T., Myoui A.: *J.R.Soc. Interface* 6, S341 (2009).
5. Scholz G., Genschow E., Pohl I., Bremer S., Paparella M., Raabe H., Southee J., Spielmann H.: *Toxicol. inVitro* 13,

- 675 (1999).
6. Laschinski G., Vogel R., Spielmann H.: *Reprod.Toxicol.* 5, 57 (1991).
7. Proff P., Romer P.: *Clin.Oral Invest.* 13, 355 (2009).
8. Bianco A., Cacciotti I., Lombardi M., Montanaro L.: *Mater. Res.Bull.* 44, 345 (2009).
9. Stauber M., Müller R.: *Meth.Mol.Biol.* 455, 273 (2008).
10. Lorensen W. E., Cline H.E.: *Computer Graphics* 21, 163 (1987).
11. Conner D.A.: *Current Protocols in Molecular Biology*, Chapter 23:Unit 23.4, John Wiley & Sons, Inc., New York 2001.
12. Winchester R. J., Ross G.: *Manual of Clinical Immunology*, p.64-76, Am. Soc. Microbiol., Washington DC 1976.
13. Mosmann T.: *J.Immunol.Meth.* 65, 55 (1983).
14. Hildebrand T., Ruegsegger P.: *J. Microsc.* 185, 67 (1997).
-